

Eur. Phys. J. A **43**, 131–136 (2010)

DOI: 10.1140/epja/i2009-10900-9

## Invariant-mass distributions for the $pp \rightarrow pp\eta$ reaction at $Q = 10$ MeV

P. Moskal, R. Czyżykiewicz, E. Czerwiński, D. Gil, D. Grzonka, L. Jarczyk, B. Kamys, A. Khoukaz, J. Klaja, P. Klaja, W. Krzemień, W. Oelert, J. Ritman, T. Sefzick, M. Siemaszko, M. Silarski, J. Smyrski, A. Täschner, M. Wolke, P. Wüstner, J. Zdebik, M.J. Zieliński and W. Zipper



Società  
Italiana  
di Fisica



Springer

## Invariant-mass distributions for the $pp \rightarrow pp\eta$ reaction at $Q = 10$ MeV

P. Moskal<sup>1,2,a</sup>, R. Czyżykiewicz<sup>1,3</sup>, E. Czerwiński<sup>1,2</sup>, D. Gil<sup>1</sup>, D. Grzonka<sup>2</sup>, L. Jarczyk<sup>1</sup>, B. Kamys<sup>1</sup>, A. Khoukaz<sup>4</sup>, J. Klaja<sup>1,2</sup>, P. Klaja<sup>1,2</sup>, W. Krzemień<sup>1,2</sup>, W. Oelert<sup>2</sup>, J. Ritman<sup>2</sup>, T. Sefzick<sup>2</sup>, M. Siemaszko<sup>3</sup>, M. Silarski<sup>1</sup>, J. Smyrski<sup>1</sup>, A. Täschner<sup>4</sup>, M. Wolke<sup>5</sup>, P. Wüstner<sup>2</sup>, J. Zdebik<sup>1</sup>, M.J. Zieliński<sup>1</sup>, and W. Zipper<sup>4</sup>

<sup>1</sup> Institute of Physics, Jagellonian University, PL-30-059 Cracow, Poland

<sup>2</sup> Nuclear Physics Institute, Research Center Jülich, D-52425 Jülich, Germany

<sup>3</sup> Institute of Physics, University of Silesia, PL-40-007 Katowice, Poland

<sup>4</sup> IKP, Westfälische Wilhelms-Universität, D-48149 Münster, Germany

<sup>5</sup> Department of Physics and Astronomy, SE-751 05 Uppsala University, Sweden

Received: 7 July 2008 / Revised: 12 October 2009

Published online: 17 December 2009 – © Società Italiana di Fisica / Springer-Verlag 2009

Communicated by P. Braun-Munzinger

**Abstract.** Proton-proton and proton- $\eta$  invariant-mass distributions and the total cross-section for the  $pp \rightarrow pp\eta$  reaction have been determined near the threshold at an excess energy of  $Q = 10$  MeV. The experiment has been conducted using the COSY-11 detector setup and the cooler synchrotron COSY. The determined invariant-mass spectra reveal significant enhancements in the region of low proton-proton relative momenta, similarly as observed previously at higher excess energies of  $Q = 15.5$  MeV and  $Q = 40$  MeV.

### 1 Introduction

The complexity of the structure of hadrons constitutes the basic difficulty in the quantitative description of the hadronic interaction in the medium-energy regime. Therefore, this interaction is not well understood especially in the meson-nucleon and meson-meson sector, where an additional difficulty is the relatively poor experimental database. Particularly challenging are investigations of interactions involving flavour-neutral mesons. This is due to the short lifetime of these mesons which can neither be used as targets nor as beams. Thus, in practice such interactions can be accessed only indirectly via observables like excitation functions or invariant-mass distributions. Measurements of these observables are especially useful in the close-to-threshold region where the final-state particles are produced with low relative velocities. Among the basic flavour neutral mesons the  $\eta$  is of particular interest since its interaction with nucleons is strong enough to be detectable with the presently achievable experimental precision [1], and since its interaction seems to be sufficiently strong to form an eta-mesic nucleus [2,3]. The existence of such kind of nuclear matter is vividly discussed [4–12] and there are ongoing experimental programs searching for a signal of such a state [13–17].

The earlier high statistics measurements of the  $pp \rightarrow pp\eta$  reaction at an excess energy of  $Q = 15.5$  MeV from the

COSY-11 Collaboration [18], and also the measurements of the TOF group [19] at  $Q = 15$  and 41 MeV, revealed that there exist significant enhancements in the invariant-mass distributions of  $pp$  and  $p\eta$  subsystems at higher values of proton-proton invariant mass and lower values of the proton- $\eta$  invariant mass. One of the plausible explanations for these enhancements could be the influence of the proton- $\eta$  interaction [1,20]. If this is the case one could use such observables for the estimation of the strength of this interaction. However, the observed invariant-mass distributions could be also plausibly explained by contributions of higher partial waves [21,22] or by an energy dependence of the primary production amplitude [23,24]. Therefore, in order to verify the correctness of the proposed explanations it is of importance to investigate the dependence of the strength of the enhancements as a function of the excess energy. Qualitatively, with decreasing excess energy the contribution from the higher partial waves should decrease whereas the influence of the interaction should be more pronounced.

Certainly, most effectively, contributions from higher partial waves could be disentangled by the determination of the analysing powers and spin transition coefficients [22,25,26], yet such investigations are not planned in the near future at COSY which is at present the only laboratory where it can be conducted. This makes the determination of the energy dependence of the distributions of the differential cross-section for the  $pp \rightarrow pp\eta$  reaction

<sup>a</sup> e-mail: p.moskal@fz-juelich.de

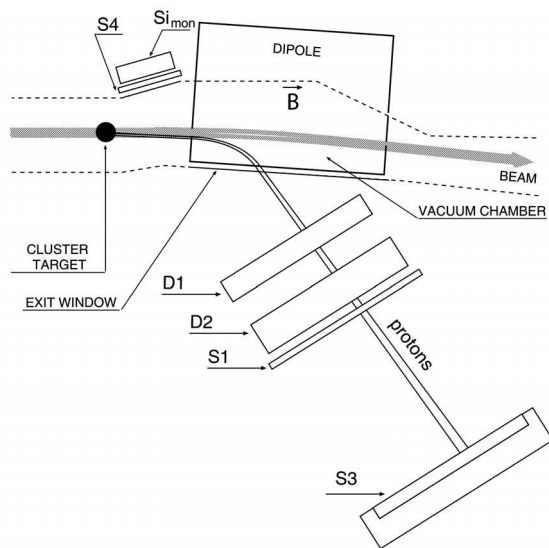


**Fig. 1.** Schematic view of the COSY-11 detector setup [30–32]. D1 and D2 represent drift chambers. S1, S3, S4 denote scintillator counters.  $Si_{mon}$  is the silicon strip detector used for the detection of the elastically scattered protons. Superimposed solid lines indicate final-state protons from the  $pp \rightarrow pp\eta$  reaction. The size of detectors and their relative distances are not to scale.

even more important for studies of the proton- $\eta$  hadronic interaction and for studies of the properties of nucleon resonances [21,27].

In this article we present distributions of the proton-proton and proton- $\eta$  invariant masses at the excess energy of  $Q = 10$  MeV which is significantly closer to the threshold with respect to the previous studies. Although the original experiment at  $Q = 10$  MeV has been devoted to the investigations of the analysing power for the  $pp \rightarrow pp\eta$  reaction [28] and has been performed with a polarised proton beam, the data enable also the determination of the spin-averaged observables after appropriate offline “depolarisation” of the beam explained in sect. 2.1. In sect. 2 we briefly describe the experimental setup, present the experimental principles of the measurement, and describe the method of the data analysis. In sect. 3 the determined spectra are compared to the analogous results determined at the excess energy of  $Q = 15.5$  MeV, and the final conclusions are drawn.

## 2 Experiment

The measurement of the  $pp \rightarrow pp\eta$  reaction has been performed at the cooler synchrotron COSY [29] at the Research Center Jülich in Germany using the COSY-11 detector setup [30–32], presented schematically in fig. 1.

The proton beam with a momentum of  $2.010$  GeV/ $c$ , corresponding to an excess energy of  $Q = 10$  MeV, has been scattered on  $H_2$  molecules from an internal cluster jet target [33,34], installed in front of the COSY magnet. Reaction products carry lower momenta than the beam protons, therefore are bent more in the magnetic field of

the dipole magnet. Positively charged ejectiles leave the scattering chamber through a thin exit window reaching the detection system operating under atmospheric pressure. The hardware trigger was based on signals from scintillator detectors only. It was adjusted to register all events with at least two positively charged particles. To this aim coincident signals in the S1 and S3 detectors were required. In the case of the S1 detector only these events were accepted for which either two separate segments were hit or an amplitude of the signal in a single module was higher than the certain threshold value. Based on the data analysis from the previous experiments, the threshold was set high enough to reduce significantly the number of single-particle events, and at the same time to accept most events (almost 100%) with two protons passing through one segment. Next, in the off-line analysis it was required that at least two tracks are reconstructed from signals measured by means of two planar drift chambers D1 and D2. The trajectories of the positively charged particles reconstructed in drift chambers are further traced through the magnetic field of the dipole back to the interaction point. In this way the momenta of the particles can be reconstructed with a precision of  $6$  MeV/ $c$  (standard deviation) [18]. The time-of-flight measurement between the scintillator hodoscope S1 and the scintillator wall S3, and the independently reconstructed momentum enable a particle identification by means of the invariant-mass technique. The COSY-11 mass resolution allows for a clear separation of groups of events with two protons, two pions, proton and pion and also deuteron and pion [1]. Further on the produced meson is identified using the missing-mass method. A more detailed description of the method and results of the identification of the  $pp \rightarrow pp\eta$  reaction can be found in refs. [1,18,35].

### 2.1 Off-line depolarisation of the beam

Originally the experiment was dedicated to the measurement of the beam analysing power for the  $pp \rightarrow pp\eta$  reaction [28,35]. Therefore, the proton beam has been vertically polarised. The vertical polarisation of the beam is defined as an asymmetry of populations of particles in the spin up ( $N_+$ ) and down ( $N_-$ ) states with respect to the vertical axis, integrated over the whole period of measurement:

$$P_y = \frac{N_+ - N_-}{N_+ + N_-}. \quad (1)$$

In the discussed experiment the direction of the polarisation was being flipped from cycle to cycle. Hence, for the so-called “spin-up cycles” we define the spin-up polarisation as

$$P^\uparrow = \frac{\sum_{i=up} n_{+,i} - \sum_{i=up} n_{-,i}}{\sum_{i=up} n_{+,i} + \sum_{i=up} n_{-,i}}, \quad (2)$$

and analogously for “spin-down cycles” the spin-down polarisation reads

$$P^\downarrow = \frac{\sum_{i=dn} n_{-,i} - \sum_{i=dn} n_{+,i}}{\sum_{i=dn} n_{-,i} + \sum_{i=dn} n_{+,i}}, \quad (3)$$

where,  $n_{+,i}$  and  $n_{-,i}$  denote the number of protons in the  $i$ -th cycle, in the spin up and down state, respectively. Please note that, according to above definitions, the following relations are valid:

$$\begin{aligned} \sum_{i=up} n_{+,i} + \sum_{i=dn} n_{+,i} &= N_+, \\ \sum_{i=up} n_{-,i} + \sum_{i=dn} n_{-,i} &= N_-. \end{aligned} \quad (4)$$

The beam can be effectively depolarized, *e.g.*, by assigning to the events in spin-up cycles the weights  $w$  which can be derived from the requirement that the numerator of eq. (1) has to vanish:

$$w \cdot \sum_{i=up} n_{+,i} + \sum_{i=dn} n_{+,i} - \left( w \cdot \sum_{i=up} n_{-,i} + \sum_{i=dn} n_{-,i} \right) = 0. \quad (5)$$

Thus, combining eqs. (2) and (3) with eq. (5) we obtain the following formula for the value of  $w$ :

$$w = \frac{P^\downarrow}{P^\uparrow} \cdot \frac{\sum_{i=dn} n_{-,i} + \sum_{i=dn} n_{+,i}}{\sum_{i=up} n_{+,i} + \sum_{i=up} n_{-,i}} = \frac{P^\downarrow}{P^\uparrow} \cdot \frac{L^\downarrow}{L^\uparrow} = \frac{P^\downarrow}{P^\uparrow} \cdot \frac{1}{L_{rel}}, \quad (6)$$

where  $L_{rel} := \frac{L^\downarrow}{L^\uparrow}$  denotes the relative luminosity for the spin up and down cycles. Taking into account the numerical values of  $P^\uparrow = 0.658 \pm 0.008$ ,  $P^\downarrow = 0.702 \pm 0.008$ , and  $L_{rel} = 0.98468 \pm 0.00056$  [28, 35] one gets  $w = 1.083$ .

The weight  $w$ , assigned to events in spin-up cycles, does not change the absolute value of cross-sections, as the same weight has been applied in both: the calculation of the number of events originating from the  $pp \rightarrow pp\eta$  reaction and the determination of the luminosity from the  $pp \rightarrow pp$  elastic scattering.

## 2.2 Data analysis

The method applied to the determination of the differential cross-sections follows the procedures described in [18], therefore for any details the reader is referred to that paper. Here we shall only briefly describe the main steps of the data analysis and emphasize the differences between the methods used in both studies.

After particle identification we continued the analysis with the depolarization of the experimental data, according to the procedure described in sect. 2.1. Next, we determined the covariance matrix and performed the kinematical fitting [1, 18].

For the description of the relative motion of the protons and the  $\eta$  meson, following ref. [18], we have chosen the squares of the invariant masses — $s_{pp}$  and  $s_{p\eta}$ — of the proton-proton and proton- $\eta$  systems, respectively. Optimizing the statistics we have divided the range of  $s_{pp}$  and  $s_{p\eta}$  into 20 bins. For each bin of these variables we have determined the spectrum of the square of the missing mass. Analogous spectra were simulated for the  $pp \rightarrow pp\eta$  reaction and for the background channels. The simulation

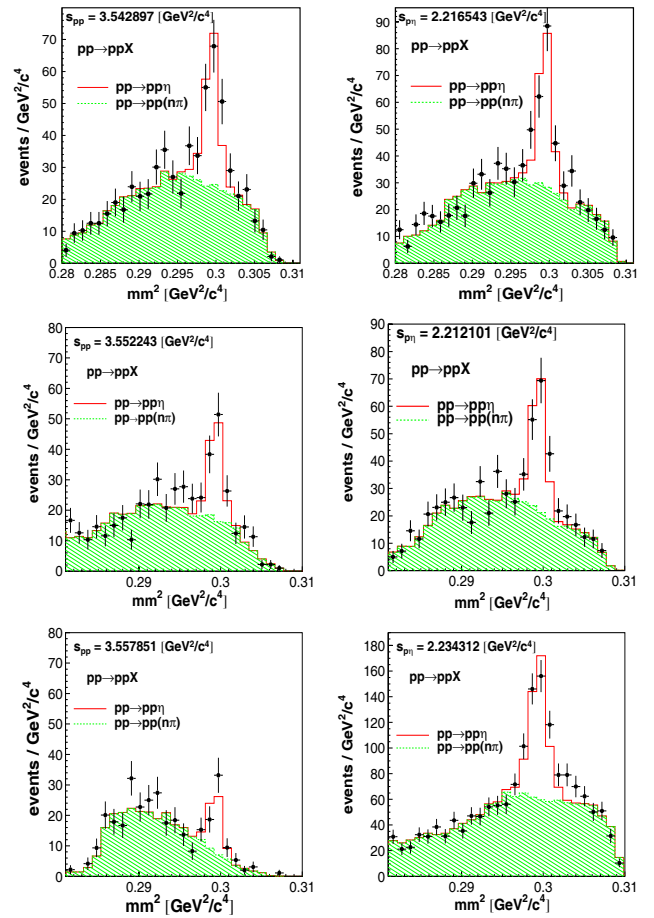


**Fig. 2.** Missing-mass-squared distributions for arbitrarily chosen bins of  $s_{pp}$  (left) and  $s_{p\eta}$  (right), as measured at the excess energy of  $Q = 10$  MeV. Dots represent the experimental data points along with their statistical errors, whereas the solid line is the best fit of the sum of the signal and background as obtained in the Monte Carlo simulations. The shaded part shows the generated multi-pionic background.

program, based on the GEANT3 [36] code, accounts for the geometry of the COSY-11 detector setup including the conditions of the beam and target [37] and the resolution and efficiency of the detectors [1]. The simulated events were analysed with the same program as the experimental data. Subsequently, functions of the type

$$f(mm^2) = \alpha \cdot f_{pp \rightarrow pp2\pi}(mm^2) + \beta \cdot f_{pp \rightarrow pp3\pi}(mm^2) + \gamma \cdot f_{pp \rightarrow pp4\pi}(mm^2) + \delta \cdot f_{pp \rightarrow pp\eta}(mm^2) \quad (7)$$

were fitted to the data, with  $\alpha$ ,  $\beta$ ,  $\gamma$ , and  $\delta$  treated as free parameters responsible for the normalisation of the simulated missing-mass spectra ( $f$ ) of the reactions indicated in the subscripts. In order to determine the background-free invariant-mass distributions the experimental missing-mass-squared spectra were fitted separately for each bin of  $s_{pp}$  and  $s_{p\eta}$ . As an example, the missing-mass distributions for arbitrarily chosen bins of  $s_{pp}$  and  $s_{p\eta}$  are presented in fig. 2.

The numbers of  $\eta$  mesons  $N_\eta$  for the individual intervals of  $s_{pp}$  and  $s_{p\eta}$  have been calculated as

$$N_\eta = \delta \cdot \int_0^{mm_{max}^2} f_{pp \rightarrow pp\eta}(mm^2) d(mm^2), \quad (8)$$

and the statistical errors  $\sigma(N_\eta)$  have been estimated as

$$\sigma(N_\eta) = \sigma(\delta) \cdot \int_0^{mm_{max}^2} f_{pp \rightarrow pp\eta}(mm^2) d(mm^2), \quad (9)$$

where  $\sigma(\delta)$  are the estimates of the  $\delta$  parameter uncertainties (standard deviations) determined by means of the MINUIT minimization package [38].

The systematic error of  $N_\eta$  has been estimated to be not larger than 8%, based on the dependence of the results on different assumptions for i) the background estimation ( $\sim 2\%$ ), ii) the description of the proton-proton final-state interaction ( $\sim 5\%$ ), and iii) the inaccuracy in efficiency for the reconstruction of both proton trajectories ( $\sim 6\%$ ). The uncertainty in the number of the background events under the peak of the  $\eta$  meson was estimated as differences between results obtained by fitting to the background a) the first-order polynomials, b) the second-order polynomials, c) the sum of two Gaussian functions, and d) the distributions simulated for the multi-pion production [39,35]. The inaccuracy due to the model used for the description of the proton-proton FSI was estimated conservatively as a difference in results determined when using the parameterization of the proton-proton  $S$ -wave interaction [40] and when neglecting the FSI and taking into account a homogeneous phase-space distribution of the momenta of final-state particles.

The determination of the luminosity was based on the comparison of the measured differential  $pp \rightarrow pp$  elastic scattering cross-sections to the data of the EDDA group [41]. For the detailed method of the luminosity and acceptance calculation the interested reader is referred to [1,37]. The integrated luminosity was extracted to be  $L = 58.53 \pm 0.03 \text{ nb}^{-1}$ .

### 3 Results and conclusions

The total cross-section evaluated as an integral of the  $s_{pp}$  distribution equals to  $\sigma = 1.27 \pm 0.04 \pm 0.13 \mu\text{b}$ , where the first error is the statistical and the second the systematic one. The latter accounts for the quadratic sum of independent contributions from 8% systematic error of  $N_\eta$ , 3% systematic error of the luminosity determination [18], and 6% uncertainty in the acceptance estimation [18]. The determined total cross-section is in line with the previous measurements performed independently by various experimental groups [18,42–47].

The results on the differential cross-sections for the  $pp \rightarrow pp\eta$  reaction as a function of the square of the proton-proton and proton- $\eta$  invariant masses are given in table 1, and presented in the left part of fig. 3. They are compared with the differential cross-sections measured at

**Table 1.** Distribution of the square of the invariant mass of the proton-proton and proton- $\eta$  systems for the  $pp \rightarrow pp\eta$  reaction at the excess energy of  $Q = 10 \text{ MeV}$ .

$s_{pp} \left[ \frac{\text{GeV}^2}{c^4} \right]$	$\frac{d\sigma}{ds_{pp}} \left[ \frac{\mu\text{b}}{\text{GeV}^2/c^4} \right]$	$s_{p\eta} \left[ \frac{\text{GeV}^2}{c^4} \right]$	$\frac{d\sigma}{ds_{p\eta}} \left[ \frac{\mu\text{b}}{\text{GeV}^2/c^4} \right]$
3.522337	$33.6 \pm 2.9$	2.207658	$11.0 \pm 2.3$
3.524206	$64.3 \pm 4.4$	2.209139	$14.6 \pm 3.2$
3.526075	$58.8 \pm 4.9$	2.210620	$24.0 \pm 4.1$
3.527944	$46.1 \pm 4.8$	2.212101	$32.4 \pm 4.8$
3.529813	$38.6 \pm 4.7$	2.213582	$32.0 \pm 5.1$
3.531682	$37.2 \pm 4.9$	2.215062	$25.4 \pm 5.1$
3.533552	$40.3 \pm 4.9$	2.216543	$51.5 \pm 6.8$
3.535421	$39.9 \pm 5.0$	2.218024	$32.1 \pm 6.0$
3.537290	$35.8 \pm 4.9$	2.219505	$50.7 \pm 6.8$
3.539159	$40.2 \pm 5.3$	2.220985	$47.2 \pm 6.7$
3.541028	$31.3 \pm 5.1$	2.222466	$57.1 \pm 7.2$
3.542897	$37.9 \pm 5.6$	2.223947	$55.9 \pm 7.2$
3.544767	$26.2 \pm 5.3$	2.225428	$60.1 \pm 7.0$
3.546636	$26.0 \pm 5.4$	2.226908	$67.4 \pm 7.4$
3.548505	$30.8 \pm 5.4$	2.228389	$67.4 \pm 6.9$
3.550374	$23.2 \pm 5.4$	2.229870	$58.5 \pm 6.3$
3.552243	$26.6 \pm 4.8$	2.231351	$56.6 \pm 5.4$
3.554112	$25.1 \pm 4.7$	2.232831	$52.9 \pm 4.6$
3.555982	$9.8 \pm 4.0$	2.234312	$41.8 \pm 3.7$
3.557851	$7.7 \pm 1.9$	2.235793	$19.0 \pm 2.0$

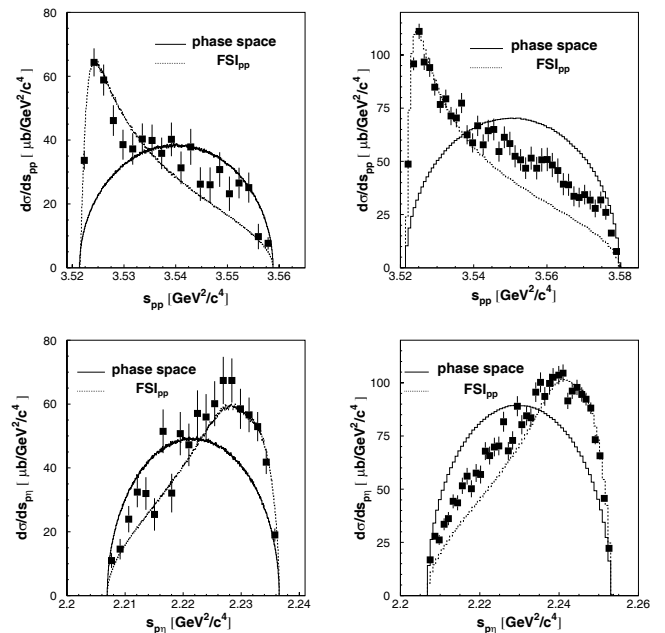


**Fig. 3.** Distributions of the square of the proton-proton and proton- $\eta$  invariant masses as measured at  $Q = 10 \text{ MeV}$  (left) and  $Q = 15.5 \text{ MeV}$  (right). Solid lines represent the homogeneous phase-space distributions, while the dotted lines are the theoretical predictions taking into account the  $^1S_0$  proton-proton final-state interaction.

the excess energy of  $Q = 15.5$  MeV [18], displayed in the right part of fig. 3.

The homogeneous phase-space distributions, shown in fig. 3 by solid lines, completely disagree with the experimental data for all distributions presented. The peak observed at small values of  $s_{pp}$  is associated with strong proton-proton final-state interaction (FSI). On the other hand the dotted lines, which represent the phase-space distribution convoluted with the proton-proton FSI describe the data quite well in the range of small invariant masses of the proton-proton system and in the range of large  $s_{pp}$ , but for both excess energies there is a significant deviation of the theoretical predictions from the experimental data in the range of large values of  $s_{pp}$  and small values of  $s_{p\eta}$ . In the calculations we have used the parameterization of the proton-proton FSI given in ref. [48]. The curves including the proton-proton FSI have been arbitrarily normalized in the range of small values of  $s_{pp}$  and close to the upper limit of the  $s_{p\eta}$  distribution.

A preliminary result from a comparative analysis of the  $pp\eta$  and  $pp\eta'$  system indicates that the observed enhancement is rather not due to the meson-proton interaction [49, 39]. Preliminary results show that the enhancements in the invariant-mass distributions are also present in the case of the  $pp \rightarrow pp\eta'$  reaction [49, 39]. Due to the fact that the interaction between the  $\eta'$  meson and the proton is more than an order of magnitude weaker than the one between the  $\eta$  meson and the proton [40], the explanation that the bump is caused by the proton- $\eta$  final-state interactions is rather dubious.

One plausible explanation for the bumps observed at higher values of  $s_{pp}$  and lower values of  $s_{p\eta}$  is the presence of higher partial waves in the final-state proton-proton system [22]. Already the inclusion of the  $^1S_0 \rightarrow ^3P_0s$  [50] transition to the production amplitude of the  $pp \rightarrow pp\eta$  reaction leads to a quite well description of the experimental data in the high values of  $s_{pp}$  and low values of  $s_{p\eta}$ , leaving unaltered the description of the experimental data at low values of  $s_{pp}$  and high values of  $s_{p\eta}$ , dominated mainly by the  $^3P_0 \rightarrow ^1S_0s$  transition. However, to cope the  $P$ -wave contribution with the flat angular distributions [18, 19], it is necessary that the amplitude  $^1D_2 \rightarrow ^3P_2s$  vanishes or that it interferes destructively with  $^1S_0 \rightarrow ^3P_0s$  transition [23]. Moreover, the model calculations based on a significant  $P$ -wave contribution underestimates the excitation function for the  $pp \rightarrow pp\eta$  reaction below 20 MeV by a factor of about two [1, 18]. Although this deficit can be overcome when assuming a relatively strong contribution to the production amplitude from the nucleon resonances, such hypothesis cannot be confirmed at the present stage of the inaccuracies of the resonance parameters [21]. The amount of the  $P$ -wave contribution should decrease towards threshold but the enhancement observed at  $Q = 10$  MeV is rather of the same order as the one at  $Q = 15.5$  MeV; however, in view of the present experimental statistical and systematic inaccuracies, the hypothesis of the higher partial-wave contribution cannot be excluded.

Another explanation for the bumps observed at higher values of  $s_{pp}$  were put forward by Deloff [23] who explains

the observed spectra by allowing a linear energy dependence of the leading  $^3P_0 \rightarrow ^1S_0s$  partial-wave amplitude. Recently also Ceci, Švarc and Zauner [24, 51] have shown that the excitation function and the enhancement in the invariant-mass spectra can be very well described by the energy dependence of the production amplitude when the negative interference between the  $\pi$  and the  $\eta$  meson exchange amplitudes is assumed. However, for the quantitative confirmation of these hypotheses still more precise data on the energy dependence of the enhancement in the invariant-mass spectra are required.

The work was partially supported by the European Community-Research Infrastructure Activity under the FP6 programme (Hadron Physics, RII3-CT-2004-506078), by the Polish Ministry of Science and Higher Education under grants Nos. 3240/H03/2006/31 and 1202/DFG/2007/03, by the German Research Foundation (DFG), and by the FFE grants from the Research Center Jülich.

## References

1. P. Moskal, arXiv: hep-ph/0408162 (Jagiellonian University Press, 2004).
2. Q. Haider, L.C. Liu, Phys. Lett. B **172**, 257 (1986).
3. G.L. Li *et al.*, Phys. Lett. B **195**, 515 (1987).
4. Q. Haider, L.C. Liu, Acta Phys. Pol. Suppl. **2**, 121 (2009).
5. A. Sibirtsev *et al.*, Phys. Rev. C **70**, 047001 (2004).
6. T. Inoue, E. Oset, Nucl. Phys. A **710**, 354 (2002).
7. Q. Haider, L.C. Liu, Phys. Rev. C **66**, 045208 (2002).
8. C. Wilkin, Phys. Rev. C **47**, R938 (1993).
9. S. Wycech *et al.*, Phys. Rev. C **52**, 544 (1995).
10. C. Hanhart, Phys. Rev. Lett. **94**, 049101 (2005).
11. S.D. Bass, A.W. Thomas, Phys. Lett. B **634**, 368 (2006).
12. V.A. Tryasuchev, A.V. Isaev, e-Print: arXiv:0901.3242.
13. W. Krzemien *et al.*, Acta Phys. Pol. Suppl. **2**, 141 (2009).
14. W. Krzemien *et al.*, Int. J. Mod. Phys. A **24**, 576 (2009).
15. B. Krusche, I. Jaegle, Acta Phys. Pol. Suppl. **2**, 51 (2009).
16. M. Pfeiffer *et al.*, Phys. Rev. Lett. **92**, 252001 (2004).
17. J. Smyrski *et al.*, Acta Phys. Pol. Suppl. **2**, 133 (2009).
18. P. Moskal *et al.*, Phys. Rev. C **69**, 025203 (2004).
19. M. Abdel-Bary *et al.*, Eur. Phys. J. A **16**, 127 (2003).
20. A. Fix, H. Arenhövel, Phys. Rev. C **69**, 014001 (2004).
21. K. Nakayama *et al.*, Acta Phys. Pol. Suppl. **2**, 23 (2009).
22. K. Nakayama *et al.*, Phys. Rev. C **68**, 045201 (2003).
23. A. Deloff, Phys. Rev. C **69**, 035206 (2004).
24. S. Ceci, A. Švarc, B. Zauner, Acta Phys. Pol. Suppl. **2**, 157 (2009).
25. H.O. Meyer *et al.*, Phys. Rev. C **63**, 064002 (2001).
26. C. Hanhart, Phys. Rep. **397**, 155 (2004).
27. K. Nakayama *et al.*, e-Print: arXiv:0803.3169.
28. R. Czyżykiewicz *et al.*, Phys. Rev. Lett. **98**, 122003 (2007).
29. D. Prasuhn *et al.*, Nucl. Instrum. Methods A **441**, 167 (2000).
30. S. Brauksiepe *et al.*, Nucl. Instrum. Methods A **376**, 397 (1996).
31. P. Klaja *et al.*, AIP Conf. Proc. **796**, 160 (2005).
32. J. Smyrski *et al.*, Nucl. Instrum. Methods A **541**, 574 (2005).
33. H. Dombrowski *et al.*, Nucl. Instrum. Methods A **386**, 228 (1997).

34. A. Khoukaz *et al.*, Eur. Phys. J. D **5**, 275 (1999).
35. R. Czyżykiewicz, PhD Thesis, Jagellonian University (2007); e-Print: nucl-ex/0702010.
36. CERN Program Libraries Long Writeups W5013 (1994).
37. P. Moskal *et al.*, Nucl. Instrum. Methods A **466**, 448 (2001).
38. MINUIT - Minimization Package, CERN Program Library Long Writeups D506 (1994).
39. P. Klaja, PhD Thesis, Jagiellonian University (2009); e-Print: arXiv:0907.1491.
40. P. Moskal *et al.*, Phys. Lett. B **482**, 356 (2000).
41. D. Albers *et al.*, Phys. Rev. Lett. **78**, 1652 (1997).
42. J. Smyrski *et al.*, Phys. Lett. B **474**, 182 (2000).
43. A.M. Bergdolt *et al.*, Phys. Rev. D **48**, 2969 (1993).
44. E. Chiavassa *et al.*, Phys. Lett. B **322**, 270 (1994).
45. H. Calén *et al.*, Phys. Lett. B **366**, 39 (1996).
46. H. Calén *et al.*, Phys. Rev. Lett. **79**, 2642 (1997).
47. F. Hibou *et al.*, Phys. Lett. B **438**, 41 (1998).
48. B.L. Druzhinin *et al.*, Z. Phys. A **359**, 205 (1997).
49. P. Klaja *et al.*, Acta Phys. Pol. Suppl. **2**, 45 (2009).
50. Following the conventional notation [25] the partial-wave states are denoted as  $^{2S+1}L_J \rightarrow ^{2S'+1}L'_J l'$ , where  $S$ ,  $L$ , and  $J$  denote the total spin, relative orbital momentum, and the total angular momentum of the  $pp$  system, respectively.  $l'$  denotes the orbital angular momentum of the produced meson.
51. S. Ceci, A. Švarc, B. Zauner, Phys. Scr. **73**, 663 (2006).